

Computational Modeling of T cell Receptor Signaling Network in Formalism of Ligand-Binding Reception

Michael Fang

Stevens Institute of Technology
mfang2@stevens.edu

Yifan Wang

Stevens Institute of Technology
ywang291@stevens.edu

ABSTRACT

Cancer Immunology focuses on the use of the immune system to combat cancers with high specificity and to provide durable, long-term immunity from such diseases. A key component of this system is the T-cell Receptor. Therefore, understanding and modeling the receptor's kinetics may prove to be useful in future attempts to control its varied and important downstream factors. The computational model on signaling network would help us fully understand the receptor communication mechanism and potentially inspire the machine-recognizable model for finding propitious ligand-binding. In this project, we developed a biochemical stochastic pi-calculus model in COMplex PATHway SIMulator(simulator). It provides more quantitative lens and clear understanding on the complex pathway processes of biochemical transactions.

KEYWORDS

T cell receptor, cellular signal communication, dynamic signaling pathway, Computational Models, ligand-binding, Mathematical model, stochastic pi-calculus

1 BACKGROUND

The Immune System in Humans and most jawed vertebrates can be arbitrarily divided into Innate and Adaptive immune systems. As their names suggest, the Innate system is an evolutionarily older system that offers protection via cytokines, removal of foreign substances in blood and lymph tissue, activation of complement cascades, and activation of the Adaptive immune system. The Adaptive Immune System, also known as the Acquired Immune System, is the system that allows an organism to develop acquired immunity of a disease after subsequent encounters with the pathogen.

The T Lymphocyte is a class of cell found in the Adaptive Immune System, named after the Thymus, where the cell line matures. Within the Thymus, c-kit+Sca1+ hematopoietic stem cells are 'trained' to be 'positively' selected and reactive against a foreign agent but also 'negatively' selected and not reactive towards self-presenting cells. Mature T-cells must pass both selection tests to be both effective against disease but not deadly towards the organism itself. Approximately 98% of immature T-cells fail these stringent requirements and die from the lack of a mitogenic (survival) signal (Starr et al.).

Those T-cells that survive selection can thereafter be classified by its functions. Briefly, they are: Helper CD4+ cells: These cells are integral in the process of helping other lymphocytes, such as B cells, mature, and for tagging and activation of cytotoxic T cells. Cytotoxic CD8+ Cells: these cells destroy virus-infected and tumor cells. Memory T cells: these cells maintain the particular selection features that allow subsequent T-cells to develop the correct specificity

against a particular disease, thereby allowing the immune system to gain immunity to novel diseases. Finally, Regulatory CD4+ cells are involved in the maintenance of immunological tolerance, such as ending an immune response once the target disease has abated. In each of these cases, the T-cell is distinguished from other lymphocytes by the presence of the T-Cell Receptor. The T-Cell Receptor (TCR) comprises of two chains, Alpha and Beta, that together attach to a foreign antigen. This event, coupled temporally closely with CD4, begins a cascade of reactions that ultimately affects transcription and translation of new proteins.

The pathway of the signal transduction from the T-Cell Receptor

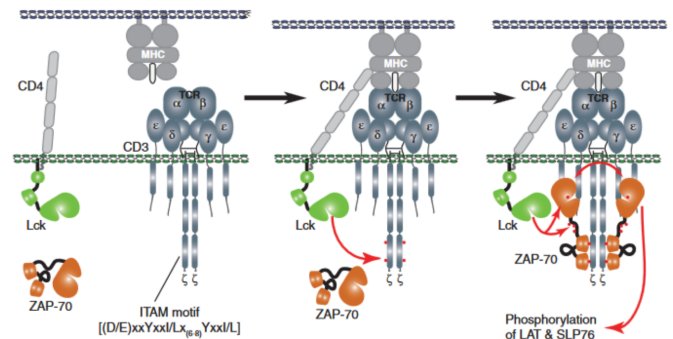


Figure 1

down to the nucleus of the T-cell is described in Figure2:

The key message here is that each depicted molecule is in-of-itself part of a number of cycles and reaction chains that are not depicted. More specifically for the purposes of modeling the kinetics is that there are many competing and possibly inhibiting reactions that are not depicted and/or not described. Therefore, the modeling carried out below should be seen as an exercise in demonstration, not as a reliable resource.

Importantly, the kinetics involved in the SLP76 complex are not well elucidated; it would be premature to make assumptions of possible rates involved.

There are two sections of the T-Cell Receptor (TCR) reaction chain whose kinetics are better known: the phosphoinositide cascade reactions as well as the MAPK/ERK pathway. Again, however, we must add a word of caution: the reaction kinetics for these pathways were not taken from T-cells and we are substituting them here because their pathways are similar. Therefore the resulting model may not be, and is probably not, indicative of in

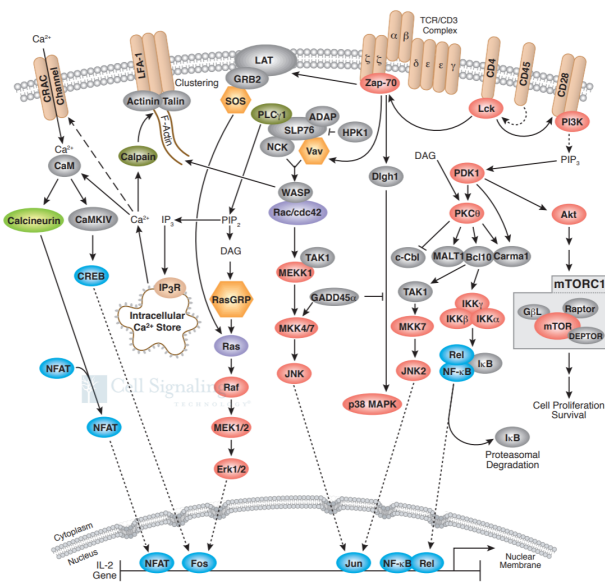


Figure 2

vivo reaction kinetics.

2 MODEL DESCRIPTION

There are two sections of the T-Cell Receptor (TCR) reaction chain whose kinetics are better known: the phosphoinositide cascade reactions as well as the MAPK/ERK pathway. Again, however, we must add a word of caution: the reaction kinetics for these pathways were not taken from T-cells and we are substituting them here because their pathways are similar. Therefore the resulting model may not be, and is probably not, indicative of in vivo reaction kinetics.

The Reactions were as listed in following. From Figure 3 to Figure 12, they are showing for the phosphoinositide cascade in separated interest reaction groups(Ref:(EECS-2007, p.38). In these reactions lists, X is representing irreversible reactions and "→" is representing multiple steps. (EECS-2007, p.38)

For the MAPK/ERK pathway we used the model from PurutÄguoÅşlu et al., which is described as a 39-step cascade. These 39 transactions are listed in Figure 13 and Figure 14.

Reaction	Kf	Kr
PLCb3 + Ca2+ ↔ PLCb3-Ca2+	20	8
Gaq-GTP + PLCb3-Ca2+ ↔ PLCb3-Ca2+-Gaq-GTP	50	0.1
PLCb3-Ca2+-Gaq-GTP + PIP2 ↔ PLCb3-Ca2+-Gaq-GTP-PIP2	70.88	1
PLCb3-Ca2+-Gaq-GTP-PIP2 → PLCb3-Ca2+ + Gaq-GDP + IP3 + DAG	27.90	X

Figure 3: IP3 synthesis by Gaq, activated by PLCb3

Reaction	Kf	Kr
Gby + PLCb3-CA2+ ↔ PLCb3-CA2+-Gby	8.35	0.39
PLCb3-CA2+-Gby + PIP2 ↔ PLCb3-CA2+-Gby-PIP2	165.83	8
PLCb3-CA2+-Gby-PIP2 → PLCb3-CA2+-Gby + IP3 + DAG	5.42	X

Figure 4: Phosphoinositide Cascade Reactions/Gby and PLCb3 reactions

Reaction	Kf	Kr
PLCb4 + Ca2+ ↔ PLCb4-Ca2+	20	8
Gaq-GTP + PLCb4-Ca2+ ↔ PLCb4-Ca2+-Gaq-GTP	62.55	10.63
PLCb4-Ca2+-Gaq-GTP + PIP2 ↔ PLCb4-Ca2+-Gaq-GTP-PIP2	1238.79	1
PLCb4-Ca2+-Gaq-GTP-PIP2 → PLCb4-Ca2+-Gaq-GDP + IP3 + DAG	22.85	X

Figure 5: Gaq and PLCb4 reactions

Reaction	Kf	Kr
IP3R + IP3 ↔ IP3R-IP3	177.47	2.2
IP3R-IP3 + Ca2+ ↔ IP3R-IP3-Ca2+	0.411	0.0434
IP3R + Ca2+ ↔ IP3R-Ca2+	0.9	0.806
IP3R-Ca2+ + IP3 ↔ IP3R-IP3-Ca2+	20	0.029233

Figure 6: IP3 receptor (IP3R) reaction rates

Reaction	Kex	Vex
3 Na+ in, 1 Ca 2+ out, Km ~2-5uM	0.25uM	0.023uM/s

Figure 7: ATPase Pumps and Na+/Ca2+ exchangers

Reaction	Kf	Kr
PKC + DAG ↔ PKC-DAG	100	0.05
PKC-DAG + Ca2+ ↔ PKC-DAG-Ca2+	10	6
PKC + Ca2+ ↔ PKC-Ca2+	0.01	30
PKC-Ca2+ + DAG ↔ PKC-DAG-Ca2+	1000	0.0001

Figure 8: Protein Kinase C reaction

3 EXPERIMENTAL RESULTS

For the phosphoinositide cascade, the the intermediary product, IP3, is rapidly produced and then consumed to activate IP3 sensitive Ca2+ channels, whereas the amount of Ca2+ ion remains relatively stable. That is, influx of Ca2+ from the endoplasmic reticulum is being bound to Protein Kinase C (PKC). The increase in diacylglycerol (DAG) would be reduced if its downstream targets involving Protein Kinase C (PKC) were extended.

In comparison to the IP3/DAG cycle, the MAPK/ERK pathway is one-directional and involves multiple amplifications of the signal,

Reaction	Kf	Kr
PKC-DAG-Ca2+ + PLCb3-CA2+ $\xrightarrow{\text{6}}$ PKC-DAG-Ca2+-PLCb3-Ca2+	830.44	111
PKC-DAG-Ca2+-PLCb3-CA2+ \rightarrow PKC-DAG-Ca2+ + PLCb3p-Ca2+	11.70/s	X
PKC-DAG-Ca2+ + PLCb4-CA2+ $\xrightarrow{\text{6}}$ PKC-DAG-Ca2+-PLCb4-Ca2+	5.90	11
PKC-DAG-Ca2+-PLCb4-Ca2+ \rightarrow PKC-DAG-Ca2+ + PLCb4p-Ca2+	0.93/s	X

Figure 9: PLCb phosphorylation by PKC rate constants

Reaction	Kf	Kr
PKC-DAG-Ca2+ + GRK $\xrightarrow{\text{6}}$ PKC-DAG-Ca2+-GRK	77.52	10
PKC-DAG-Ca2+-GRK \rightarrow PKC-DAG-Ca2+ + GRKp	18.34/s	X
<u>GRKp</u> + <u>Gby</u> $\xrightarrow{\text{6}}$ <u>GRKp-Gby</u>	4.98	0.05
GRKp-Gby + C5aC $\xrightarrow{\text{6}}$ GRKp-Gby-C5aC	591.54	12.37
GRKp-Gby-C5aC \rightarrow GRKp-Gby + C5aCp	199.31/s	

Figure 10: G-protein Receptor Kinase (GRK) activation/phosphorylation

Reaction	Kf	Kr
PLCb3p-Ca2+ \rightarrow PLCb3-CA2+	0.12/s	X
PLCb4p-Ca2+ \rightarrow PLCb4-CA2+	0.12/s	X
C5aCp \rightarrow C5aR + C5a	0.001	X

Figure 11: Dephosphorylation problems

Reaction	Vmax/Kf	Km/Kr
DAG \rightarrow null	0.35/s	
IP3 + IP3Ka \rightleftharpoons IP4 + IP3Ka	13.9	0.0557
IP4 \rightleftharpoons IP5	100	1.4
IP5 \rightarrow PIP2	0.008	

Figure 12: DAG degradation/dephosphorylation

- (1) Grb2 + SOS \rightarrow Grb2-SOS
- (2) EGFR + Shc + Grb2-SOS \rightarrow EGFR + Shc-Grb2-SOS_m
- (3) EGFR + Grb2-SOS \rightarrow EGFR + Grb2-SOS_m
- (4) Shc-Grb2-SOS_m \rightarrow Shc + Grb2-SOS
- (5) Grb2-SOS \rightarrow Grb2 + SOS
- (6) Shc-Grb2-SOS_m + Ras.GDP \rightarrow Shc-Grb2-SOS_m + Ras.GTP
- (7) Grb2-SOS_m + Ras.GDP \rightarrow Grb2-SOS_m + Ras.GTP
- (8) Ras.GTP \rightarrow Ras.GDP
- (9) GAP + Ras.GTP \rightarrow GAP + Ras.GDP

Figure 13: MAPK/ERK pathway Part1

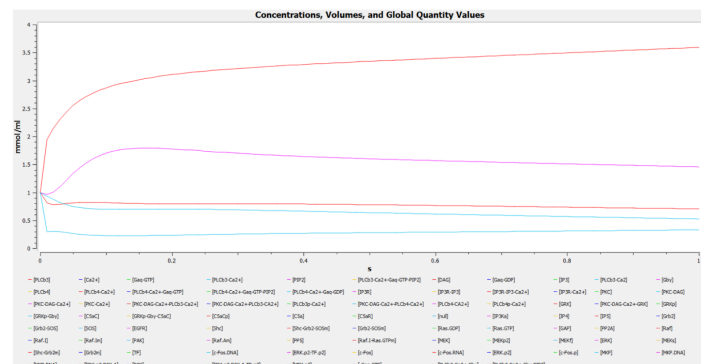
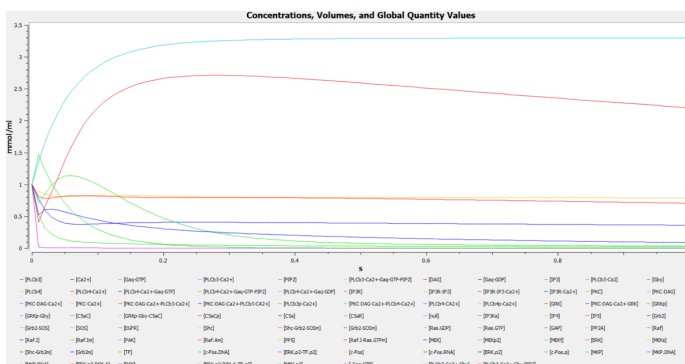
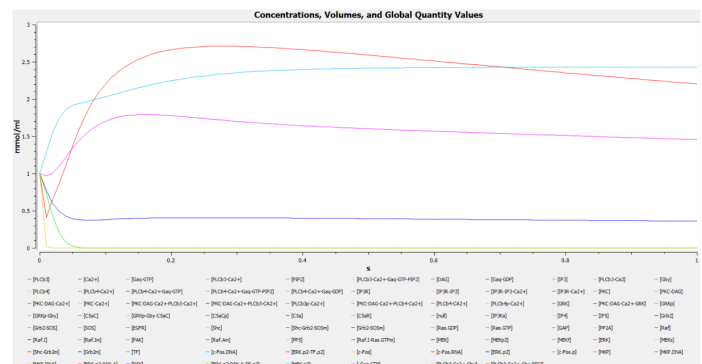
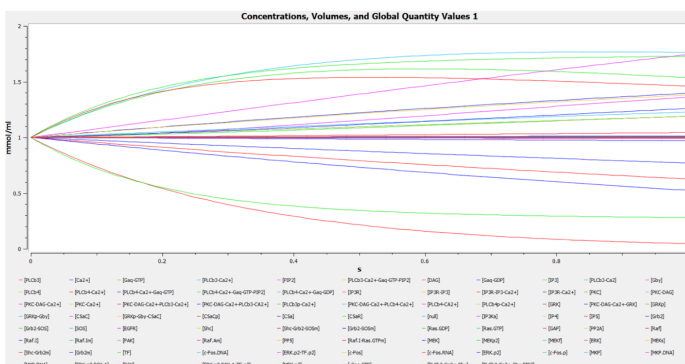
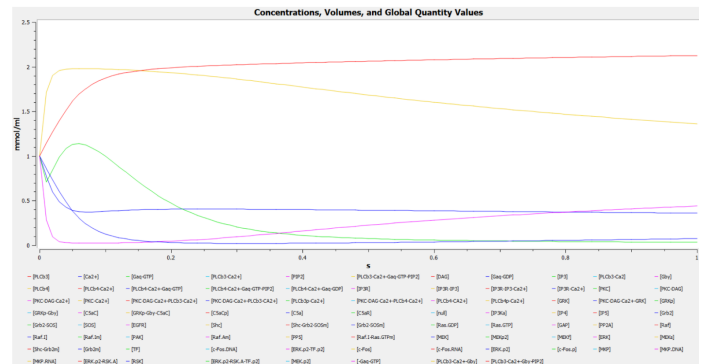
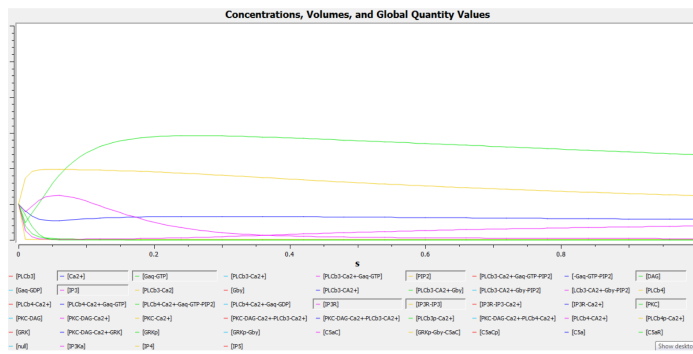
- (10) Raf + PP2A \rightarrow Raf.I + PP2A
- (11) Raf.I + Ras.GTP \rightarrow Raf.I_m + Ras.GTP
- (12) Raf.I_m + Ras.GTP + PAK \rightarrow Raf.A_m + Ras.GTP + PAK
- (13) PP5 + Raf.A_m \rightarrow PP5 + Raf.I_m
- (14) Raf.I_m \rightarrow Raf
- (15) Raf.I-Ras.GTP_m \rightarrow Raf.I_m + Ras.GTP
- (16) Raf.A_m + MEK \rightarrow Raf.A_m + MEK.p2
- (17) PAK + MEK \rightarrow PAK + MEK_F
- (18) MEK_F + Raf.A_m \rightarrow MEK.p2 + Raf.A_m
- (19) MEK.p2 + ERK \rightarrow MEK.p2 + ERK.p2
- (20) ERK.p2 + MEK \rightarrow ERK.p2 + MEK_S
- (21) MEK_S + Raf.A_m \rightarrow MEK.p2 + Raf.A_m
- (22) ERK.p2 + Shc-Grb2-SOS_m \rightarrow ERK.p2 + Shc-Grb2_m + SOS
- (23) ERK.p2 + Grb2-SOS_m \rightarrow ERK.p2 + Grb2_m + SOS
- (24) Shc-Grb2_m \rightarrow Shc + Grb2
- (25) Grb2_m \rightarrow Grb2
- (26) ERK.p2 + TF \rightarrow ERK.p2-TF.p2
- (27) ERK.p2-TF.p2 + c-Fos.DNA \rightarrow ERK.p2-TF.p2 + c-Fos.DNA + c-Fos.RNA + c-Fos
- (28) ERK.p2 + c-Fos \rightarrow ERK.p2 + c-Fos.p
- (29) ERK.p2-TF.p2 + MKP.DNA \rightarrow ERK.p2-TF.p2 + MKP.DNA + MKP.RNA + MKP
- (30) MKP + ERK.p2 \rightarrow MKP + ERK
- (31) ERK.p2 + RSK \rightarrow ERK.p2-RSK.A
- (32) ERK.p2-RSK.A + TF \rightarrow ERK.p2-RSK.A-TF.p2
- (33) ERK.p2-RSK.A-TF.p2 + c-Fos.DNA \rightarrow ERK.p2-RSK.A-TF.p2 + c-Fos + c-Fos.DNA + c-Fos.RNA
- (34) ERK.p2-RSK.A + c-Fos \rightarrow ERK.p2-RSK.A + c-Fos.p
- (35) ERK.p2-RSK.A-TF.p2 + MKP.DNA \rightarrow ERK.p2-RSK.A-TF.p2 + MKP + MKP.DNA + MKP.RNA
- (36) MKP + ERK.p2-RSK.A \rightarrow MKP + ERK + RSK
- (37) ERK.p2-TF.p2 \rightarrow ERK.p2 + TF
- (38) ERK.p2-RSK.A \rightarrow ERK.p2 + RSK
- (39) ERK.p2-RSK.A-TF.p2 \rightarrow ERK.p2-RSK.A + TF

Figure 14: MAPK/ERK pathway Part2

as well as multiple targets for regulation. Thus we see that many of the reaction concentrations quickly saturate as we would expect from.

4 FUTURE WORK

This exercise in modeling describes a number of major challenges to this area of computational biology. Firstly, the interests of a physician interested in cancer immunology differs from that of the biologist studying T-cells which differ from the chemist's interest in measuring reaction kinetics. The result is that not only are there large gaps of knowledge in, say, whether or not a particular schema or level of depth is appropriate to model, but also in the fundamental understanding of which of dozens of reactions actually occur in the way they are depicted.



Secondly, these various interests and perspectives result in different values. For most biologists and physicians, any particular reaction chain's kinetics is not all that important; only the slowest rate, known as the limiting rate, really matters. Everything else occurs faster, often many magnitudes faster, and thus are ignored. There are practical issues as well; many reaction kinetics determined in vitro are based on either non-human or, in the case of cancer research, otherwise specific cell lines, and that alone carries a major asterisk of not necessarily applying to a conception

of what a model for the human would look like.

Therefore, what this exercise highlights is the need to be specific and cautious when choosing a modeling topic. Because there are still such large gaps in our understanding of biology (and indeed, that is a virtue of science, given the especially personal nature of this field to our understanding of how the world works), it is necessary to focus on modeling either very narrowly on particularly well demonstrated and replicated functions or on

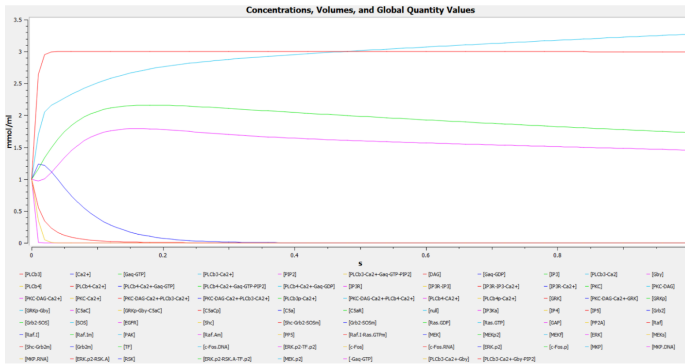


Figure 21: Protein Kinase C (PKC) reactions



Figure 22: PLCb phosphorylation by PKC

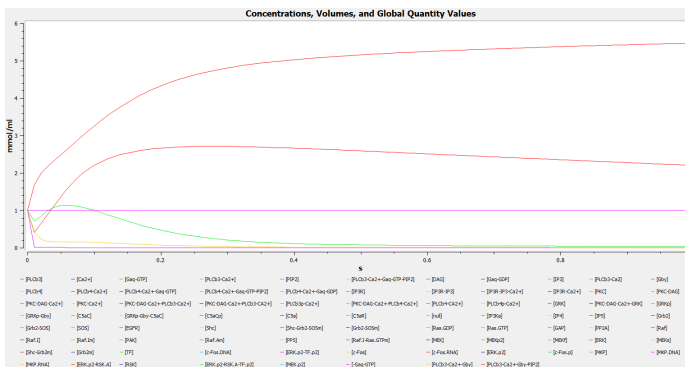


Figure 23: DAG degradation and dephosphorylation

higher level abstractions.

5 REFERENCE

[1]Bu JY, Shaw AS, Chan AC. Analysis of the interaction of ZAP-70 and syk protein-tyrosine kinases with the T-cell antigen receptor by plasmon resonance. *Proc Natl Acad Sci U S A*. 1995 May 23;92(11):5106-10.

Jinsung Hong, Stephen P. Persaud, Stephen Horvath, Paul M.

Allen, Brian D. Evavold and Cheng Zhu. Force-Regulated In Situ TCR-Peptide-Bound MHC Class II Kinetics Determine Functions of CD4+ T Cells. doi: 10.4049/jimmunol.1501407 *J Immunol* 2015; 195:3557-3564; Prepublished online 2 September 2015; <http://www.jimmunol.org/content/195/8/3557>

Haopeng Wang, Theresa A. Kadlecck, Byron B. Au-Yeung, Hanna E. Sjo Ī lin Goodfellow,Lih-Yun Hsu, Tanya S. Freedman, and Arthur Weiss, ZAP-70: An Essential Kinase in T-cell Signaling. Howard Hughes Medical Institute, Rosalind Russell Medical Research Center for Arthritis,Department of Medicine, University of California, San Francisco, San Francisco, California 94143

Jon C. D. Houtman, Richard A. Houghtling, Mira Barda-Saad, Yoko Toda, and Lawrence E. Samelson. Early Phosphorylation Kinetics of Proteins Involved in Proximal TCR-Mediated Signaling Pathways *J Immunol*. Author manuscript; available in PMC 2006 Mar 27.

Meirav Sela,Yaron Bogin, Dvora Beach, Thomas Oellerich, Johanna Lehne, Jennifer E Smith-Garvin, Mariko Okumura, Elina Starosvetsky, Rachelle Kosoff, Evgeny Libman, Gary Koretzky, Taku Kambayashi, Henning Urlaub, JĀijrgen Wienands, Jonathan Chernoff, and Deborah Yablonski. Sequential phosphorylation of SLP-76 at tyrosine 173 is required for activation of T and mast cells. *EMBO J*. 2011 Aug 3; 30(15): 3160ĀĀ3172.

Vilda PurutĀġuoĀġlu and Ernst Wit. Estimating Network Kinetics of the MAPK/ERK Pathway Using Biochemical Data. *Mathematical Problems in Engineering*. Volume 2012, Article ID 752631, 34 pages. <http://dx.doi.org/10.1155/2012/752631>.

Starr TK, Jameson SC, Hogquist KA (2003-01-01). "Positive and negative selection of T cells". *Annual Review of Immunology*. 21 (1): 139ĀĀ176. doi:10.1146/annurev.immunol.21.120601.141107. PMID 12414722.

Jens R. Sydor, Martin Engelhard, Alfred Wittinghofer, Roger S. Goody, and Christian Herrmann. Transient Kinetic Studies on the Interaction of Ras and the Ras-Binding Domain of c-Raf-1 Reveal Rapid Equilibration of the Complex. *Biochemistry*, 1998, 37 (40), pp 14292ĀĀ14299 DOI: 10.1021/bi980764f. Abteilung Physikalische Biochemie und Abteilung Strukturelle Biologie, Max-Planck-Institut fĀijr Molekulare Physiologie, Postfach 102664, 44026 Dortmund, Germany